



Cite this: *RSC Adv.*, 2023, 13, 25350

# A polystyrene-based ESIPT fluorescent polymeric probe for highly sensitive detection of chromium(vi) ions and protein staining†

Xiaoling Qin, Guoqiang Zhou, Pan Ma, Jiaoyun Xia, Fuchun Gong, \* Lusén Chen and Lujie Xu

A "two-step" preparation method of an excited-state intermolecular proton transfer (ESIPT) fluorescent polymer (f-PP) is reported here. The synthesis of f-PP involves the acetylation of polystyrene and a "multicomponent one pot" reaction. The as-prepared polymer bears a group of ESIPT fluorescent units, enabling it to exhibit high brightness, moderate solubility and ESIPT fluorescence. F-PP gives off tautomeric bright green fluorescence under UV-tamp and the dual-emission could be specifically suppressed by Cr(vi). This phenomenon cannot be elicited by other competing species. On this basis, an ESIPT polymeric probe-based method for the determination of Cr(vi) was developed, offering high sensitivity (19.5 nM) and selectivity. The f-PP was successfully used to detect Cr(vi) in real water samples by standard adding methods, indicating its application feasibility.

Received 24th April 2023  
Accepted 11th July 2023

DOI: 10.1039/d3ra02698a

rsc.li/rsc-advances

## 1. Introduction

The rapid development of industry has caused serious heavy metal ion contamination of the water environment and elicited strong concern throughout the world.<sup>1–3</sup> Among the heavy metal ion pollutants, the dispersion of cadmium ions is one of the most concerning environmental issues. Chromium tends to exist in two stable oxidation states in the environment, namely Cr(III) and Cr(VI). Cr(III) is an indispensable trace ion for biological processes, yet, Cr(VI) is one of the most toxic and ubiquitous pollutants to the ecosystem due to its mutagenic and carcinogenic features.<sup>4,5</sup> Some biochemical experiments demonstrated that the Cr(VI) ion was easily ingested into cells and reduced to Cr(III), which tends to generate radicals of various active species.<sup>6</sup> Once Cr(VI) is taken into the cells, it can disturb several biochemical processes in cells, which can elicit toxicity to them and result in DNA damage *via* activating DNA reaction.<sup>7</sup> As a result, the World Health Organization (WHO) has suggested the maximum allowable concentration for Cr(VI) in the ground and drinking water should not exceed 50 µg L<sup>−1</sup>, which were set by many nations.<sup>8</sup> Consequently, to develop a sensitive, simple and rapid analytical method is highly desirable for monitoring Cr(VI) in water, environmental, food and biological samples.

Many analytical methods are available for the detection of Cr(VI) in various samples. Among them, atomic absorption spectroscopy (AAS),<sup>9</sup> surface plasmon resonance (SPR),<sup>10</sup> UV-visible spectroscopy (UV-vis),<sup>11</sup> surface-enhanced Raman scattering (SERS),<sup>12</sup> high pressure liquid chromatography-inductively coupled plasma mass spectrometry (HPLC-MS),<sup>13</sup> X-ray absorption spectrometry (X-AS)<sup>14</sup> and electrochemistry (EC)<sup>15</sup> are frequently used for the detection of Cr(VI) in aqueous samples. Although the above techniques can afford high sensitivity and multi-element analysis, most of them involve complicated operating procedures and expensive equipment, which are associated with complex sample preparation and are time-consuming.<sup>16</sup> Currently, fluorescent molecular probes have drawn great attention due to their high sensitivity, instantaneous response, simplicity and low-cost.<sup>17</sup> So far, a large number of fluorescent probes including small organic small dyes,<sup>18</sup> nanostructures (for instance, organic or inorganic nanoparticles, metal nanoclusters, quantum dots, carbon dots) and fluorescent polymers have been used in the design of probes for the detection of Cr(VI).<sup>19–25</sup> However, the mentioned fluorophores are often suffered from insufficient sensitivity, cytotoxicity, complicated synthetic process, photo-bleaching or high fabrication cost. Developing new fluorescent dyes for probe application that are more sensitive, cheaper, low toxic, robust and facile for the highly selective and sensitive detection of Cr(VI) ions is still very necessary.

Compared to small molecular fluorophores, fluorescent polymers have the advantages of good stability, high fluorescence brightness, simple synthesis, and high safety. The polymeric fluorophores generally originate from the conjugated polymers (CPs) which bear conjugated main chain or π-

College of Chemistry and Chemical Engineering, Changsha University of Science and Technology, Changsha, 410114, P. R. China. E-mail: gongfc139@163.com; Tel: +86-0731-85258733

† Electronic supplementary information (ESI) available. See DOI: <https://doi.org/10.1039/d3ra02698a>



aromatic scaffolds.<sup>26,27</sup> Because of their excellent photo-physical properties, CPs have been employed for designing molecular probes for the detection of heavy metal ions or organic active molecules in the past decades.<sup>28–30</sup> CP-based probes often include two major functional units, namely conjugated backbones and functional side chains. In the polymeric probes, the backbone structures endow the probes with different intrinsic fluorescent features, offering “turn on” or “turn off” fluorescent switch during analyte recognition.<sup>31,32</sup> However, except for few polymers, such as the reported polydiacetylene and polythiophene,<sup>33,34</sup> the absorption and fluorescence spectra can alter a lot after their interaction with targets, almost polymeric fluorophores require the modification with different functional groups, including ionization of side chains, quenching groups, chromogenic dyes, and responsive units to obtain active sites for guest recognition.<sup>35,36</sup> The modified side chains may further enhance the sensing performance of probes, enabling CP-based probes to show higher sensitivity than that of small molecular probes.<sup>37,38</sup> Actually, some non-conjugated polymers such as poly(amidoamine), polyurethane, polyethylenimine, poly(ether amide) can also exhibit strong fluorescence when they come into existence in nanostructures under favorable conditions, which can be employed for the design of probes.<sup>39,40</sup> However, these nano-fluorophores usually bear a single functional group and they must be grafted with additional groups to meet the requirements of probe recognition. Such modifications usually lead to the destruction of nanostructures and discount fluorescence advantages of nano-fluorophores.

During previous efforts to construct small excited-state intermolecular proton transfer (ESIPT) fluorescent dyes,<sup>41,42</sup> we demonstrated that the ESIPT molecules can give off tautomeric emission benefited from the formation of intermolecular hydrogen bonds. In this study, a Cr(vi)-specific probe was designed and synthesized *via* simple modification of polystyrene polymers. For the preparation of ESIPT fluorescent polymers, excited-state intermolecular proton transfer (inter-ESPT) moieties were grafted to the polymers as fluorophores and recognition units, and the amino and hydroxyl groups in the ESIPT scaffolds were used to improve the solubility. The ESIPT fluorescent polymer-based probe exhibited excellent ESIPT fluorescent features and a quenching effect on Cr(vi).

## 2. Experimental section

### 2.1. Materials and instruments

All reagents and chemicals were used directly without any further purification. Polystyrene and acetyl chloride were purchased from China Pharmatech Ltd. (Shanghai, China). 4-(Diethylamino)-2-hydroxybenzaldehyde, malonitrile and ammonium acetate were obtained from Macklin (Shanghai, China). The ionic solutions were prepared by dissolving their relative sodium and chloride salts, respectively. Deionized water was employed in all experiments in this study.

The <sup>1</sup>H- and <sup>13</sup>C-NMR spectra were measured using an AV-600 spectrometer (Bruker, Switzerland) with tetramethylsilane (TMS;  $\delta = 0$  ppm) as an internal reference. The UV-visible absorption experiments were performed on a UV-1800

spectrophotometer (Shimadzu, Japan). Fluorescence spectra were obtained from an F-7000 spectrophotometer (Hitachi, Japan). The time-resolved fluorescence spectra were recorded on the transient fluorescence spectrometer (Edinburgh-FLS1000, England). The fluorescence quantum yields were measured by HORIBA FluoroMax-4P (HORIBA Jobin Yvon).

### 2.2. Synthesis of probe f-PP

As shown in Scheme 1, ESIPT fluorescent polymer (f-PP) was prepared by a two-step procedure of acetylation and “multi-component one pot” reaction. Briefly, acetyl polystyrene was synthesized using Friedel–Crafts acetylation method. The acetylated polystyrene polymers were then prepared *via* “multi-component one pot” reaction method. Details of synthesis and characterization of f-PP can be found in ESI.†

### 2.3. General spectra measurements of f-PP

The stock solution of f-PP (0.01 g L<sup>−1</sup>) was prepared by dissolving f-PP products in DMF-HEPES mixed system (20 mM, pH 7.2, 3 : 7, v/v). The Cr(vi) stock solution (0.1 M L<sup>−1</sup>) was obtained from the dissolution of 2.942 g potassium dichromate in 100 mL deionized water. The other solutions containing competitive species (0.1 M) were prepared by dissolving responsive compounds with deionized water. For the measurements of Cr(vi), different concentrations of competing metal ions or anion were introduced in the f-PP-containing solutions in portions. After 6 min-incubation at room temperature, the resulting mixtures were measured by UV-visible absorption and fluorescence spectrometry.

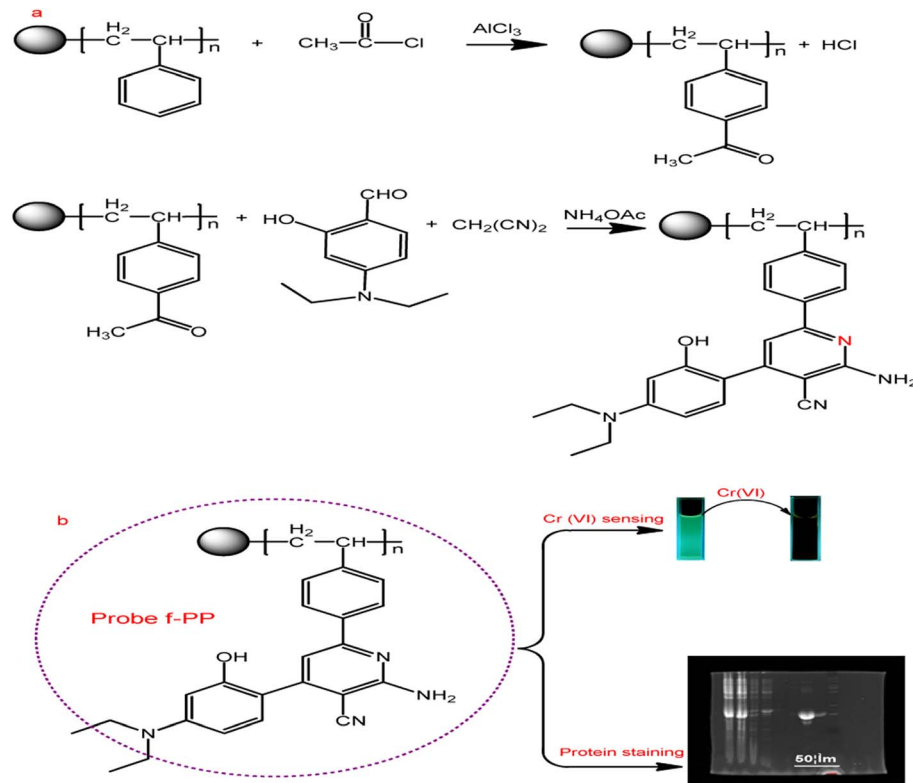
### 2.4. Detection of Cr(vi) in real water samples

The lake water and tap water were collected from our campus (Changsha, China). The wastewater was also obtained from drainage ditch in our campus. For the sample preparation, 10 mL wastewater was collected in sample tubes. These samples were then filtered three times using a 0.17  $\mu$ m membrane to reject any solid suspensions. Finally, the filtrated samples were spiked with different Cr(vi) concentrations and their fluorescence spectra were measured as above. The lake water and tap water samples were directly treated with the standard additions of Cr(vi) and the fluorescence spectra were monitored.

### 2.5. Protein staining using f-PP

The protein samples were the expressed products of Mambalgin gene and the inclusions of *Escherichia coli*, which were obtained from the State Key Laboratory of Bioorganic and Natural Products Chemistry, Shanghai Institute of Organic Chemistry, Chinese Academy of Sciences (Shanghai, China) in this study. Firstly, the proteins derived from Mambalgin gene or the protein inclusions of *Escherichia coli* were separated and fixed *via* SDS-PAGE. Next, the protein bands ([https://www.baidu.com/link?url=79xGmSk81dLifzk1gXLC9Py\\_BEf3NT0GHcZv3EHgHIB75iloig68-zvmYUjSl84NFLa2Zsi3\\_0Wkfts\\_mCTa&wd=&eqid=ec8b59280000aabbf000000066428feeb](https://www.baidu.com/link?url=79xGmSk81dLifzk1gXLC9Py_BEf3NT0GHcZv3EHgHIB75iloig68-zvmYUjSl84NFLa2Zsi3_0Wkfts_mCTa&wd=&eqid=ec8b59280000aabbf000000066428feeb)) was stained with f-PP or Coomassie brilliant blue R 250, respectively. The stained





**Scheme 1** Synthesis strategy of the ESIPT fluorescent polymeric probe f-PP and its application. (a) Synthetic route of f-PP; (b) the applications of f-PP to Cr(vi)-sensing and protein staining.

electrophoresis gel bands were then decolorized by immersing in an ethanol–water system (1 : 4, v/v) for 1 h and washed with HEPES (10 mM, pH 6.5) for three times. Finally, fluorescence scanning of the resulting electrophoresis gels was performed on a Typhoon 9410 imaging system. Coomassie brilliant blue R250 was employed as a reference to stain the same proteins. The f-PP staining solution was prepared by dissolving 0.2 mg f-PP in 5 mL DMF. When used, the f-PP-containing solution was diluted to 100 mL with a DMF–water mixed system (3/7, v/v) to obtain a 2.0  $\mu\text{g mL}^{-1}$  f-PP staining solution. 0.25% Coomassie brilliant blue R250 solution was obtained from dissolving 0.25 g Coomassie in 45 mL methanol, and followed by adding 45 mL water and 10 mL glacial acetic acid.

### 3. Results and discussion

#### 3.1. Synthesis and characterization

As shown in Scheme 1, the inter-ESIPT fluorescent polystyrene polymers (f-PP) were synthesised ([http://www.baidu.com/link?url=Ih5i62PCwBezWEGITjCZxME-10kvhcy8G8Ygz7kgfCYFG-h91-qVDLYsZxWBCiISwUVSxWtxycW5dKNGIbEV3xOp10uKv\\_3VY3YqpAxaRhG](http://www.baidu.com/link?url=Ih5i62PCwBezWEGITjCZxME-10kvhcy8G8Ygz7kgfCYFG-h91-qVDLYsZxWBCiISwUVSxWtxycW5dKNGIbEV3xOp10uKv_3VY3YqpAxaRhG)) through acetylation and “multicomponent one pot” reaction with moderate yield. The structures of the prepared f-PP have been confirmed by  $^1\text{H}$ -NMR and  $^{13}\text{C}$ -NMR (Fig. S1-1, S1-2, ESI†).

The structure of f-PP was also characterized using XPS analysis. As shown in Fig. 1 in the survey spectrum, the probe f-PP exhibits three distinct signals at 287.5, 402.5 and 534 eV,

which corresponds to C 1s, N 1s and O 1s peaks, respectively. The XPS analysis results indicated the existence of 72.1% C, 22.3% O and 5.6% N in the f-PP molecule system. Since the carbon atoms present in the probes f-PP are faced to four chemical microenvironments, four different bands at 288.53, 286.57, 284.71, and 284.41, eV can be observed in the high-resolution C 1s spectrum (Fig. 1b), attributing to the C=O/C=N, C–O, C–N, and C=C/C–C species, respectively. The high-resolution spectrum of O 1s shows three bands at 533.74, 532.77 and 531.68 eV, ascribing to C–OH/C–O–C, C–O, and C=O binding atoms, respectively. The N 1s spectrum (Fig. 1d) showed two obvious peaks at 401.057, and 399.24 eV, related to N–H, and C–N bonds, respectively.

In addition, the as-prepared ESIPT polymer was further confirmed using infrared spectrometry. It is clear that two new peak at 3265 and 1507  $\text{cm}^{-1}$  appeared in the spectrum of f-PP, ascribed to the  $-\text{NH}_2$  (connecting to benzene ring) stretching vibration compared to native acetyl polystyrene (Fig. S2a and b†). As for the spectrum of  $-\text{CN}$  groups, a distinct new peak at 2227  $\text{cm}^{-1}$  can be observed. These results imply the presence of large numbers of amino and cyano groups on the side chains of f-PP.

#### 3.2. Photophysical properties and response behavior of f-PP

In order to investigate the optical performance of f-PP, we investigated the UV-visible absorption and fluorescence spectra of f-PP. As shown in Fig. 2a three absorption bands located at



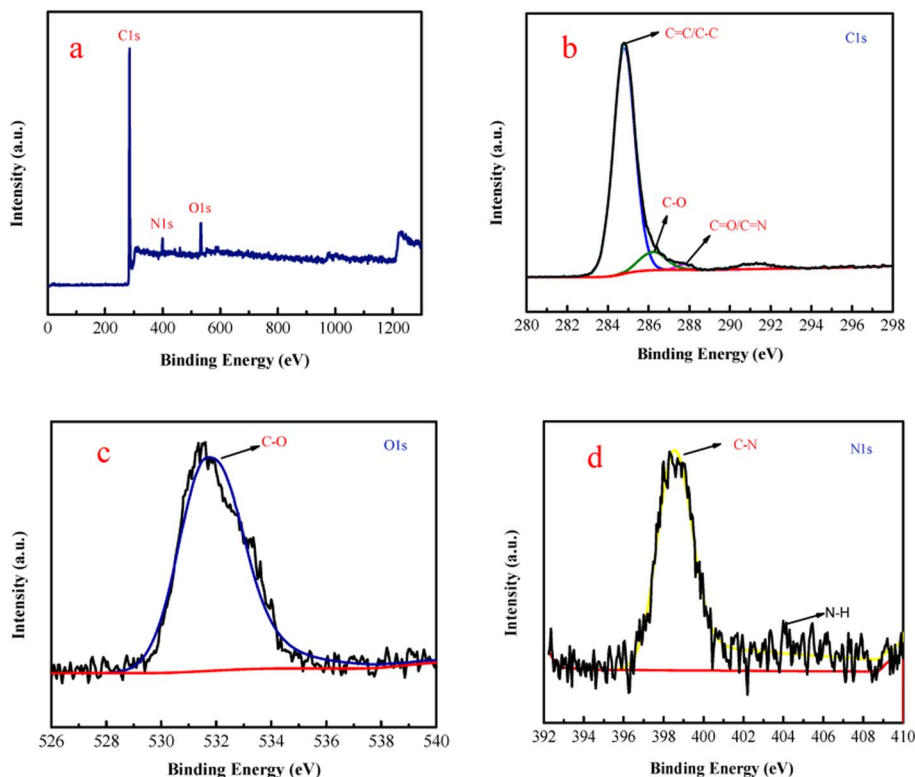


Fig. 1 (a) XPS survey spectrum of f-PP and high-resolution spectra of C 1s (b), O 1s (c), and N 1s (d).

255 nm, 355 nm and 440 nm can be observed in the UV-vis spectrum. The former two absorption bands can be assigned to the  $n\text{-}\pi^*$  transitions of the C=O bonds, and the absorption band at 440 nm can be ascribed to the  $n\text{-}\pi^*$  transition of  $p\text{-}\pi$  conjugated systems between benzenes and pyridine rings. When added with Cr(vi), the absorption peaks of f-PP containing solution increased significantly. This change in absorption spectra may generated from the aggregation of f-PP chain induced by Cr(vi), which is agree with the reported event in literature.<sup>43</sup> This result reveals that the interaction between f-PP and Cr(vi) occurred. Fluorescence spectra of f-PP indicates that there are two obvious emission peaks at 310 nm and 512 nm, in which the short wavelength fluorescence is attributed to the normal form and another one corresponding to the ESPT emission of f-PP. Upon the addition of Cr(vi), the dual-emission was obviously quenched (Fig. 2b and c). Considering that the inter-ESPT reaction is seriously affected by solvents, we evaluated the fluorescence behavior of f-PP in different solvents. As shown in Fig. 2d, f-PP exhibit normal fluorescence in conventional aprotic solvents and can give off tautomeric fluorescence in protic solvents. Surprisingly, the glacial acetic acid can also cause triple emission, implying that there is another luminescence mechanism involved. These results confirm that ESPT process of f-PP requires the assistance of solvent molecules with hydrogen receptor/donor.

To further understand the fluorescence mechanism, we monitored the fluorescent lifetime of f-PP in DMF-HEPES buffer (20 mM, pH 7.2, 3 : 7, v/v) at different emission bands. As

shown in Fig. S2c and d,<sup>†</sup> the fluorescence lifetimes of the f-PP at 310 and 512 nm are 1.176 ns and 2.714 ns, respectively. It is clear that the fluorescence decay of f-PP at 512 nm is significantly slower than that at 310 nm, which imply that the extended time may be used to undertake energy conversion between the two tautomers of f-PP.

### 3.3. Studies on the selectivity and anti-interference of f-PP

The high selectivity of probes for detecting analytes over the potentially competing species is one of the important indicators of its performance. For this purpose, the competitive measurements on Cr(vi) were used to evaluate the selectivity of the probe f-PP for Cr(vi). As shown in Fig. 3a, only Cr(vi) elicited a remarkable fluorescence quenching, whereas all conventional metal ions, including alkali, alkali-earth, transition metal ions ( $\text{K}^+$ ,  $\text{Na}^+$ ,  $\text{Ca}^{2+}$ ,  $\text{Mg}^{2+}$ ,  $\text{Ba}^{2+}$ ,  $\text{Ag}^+$ ,  $\text{Zn}^{2+}$ ,  $\text{Mn}^{2+}$ ,  $\text{Co}^{2+}$ ,  $\text{Pd}^{2+}$ ,  $\text{Hg}^{2+}$ ,  $\text{Ni}^{2+}$ ,  $\text{Cd}^{2+}$ ,  $\text{Fe}^{3+}$ ,  $\text{Cr}^{3+}$ ,  $\text{Al}^{3+}$ ,  $\text{Pr}^{3+}$ ,  $\text{Ce}^{4+}$ ) and anions ( $\text{F}^-$ ,  $\text{Cl}^-$ ,  $\text{I}^-$ ,  $\text{CO}_3^{2-}$ ,  $\text{SO}_4^{2-}$ ,  $\text{NO}_3^-$ ,  $\text{HPO}_4^{2-}$ ) merely result in negligible change in the fluorescence, even when the alkali and alkali-earth  $\text{K}^+$ ,  $\text{Na}^+$ ,  $\text{Mg}^{2+}$  and  $\text{Ca}^{2+}$  were added up to micromolar levels. The results reveal the specific oxidation of f-PP by Cr(vi) and exhibit the ability to specially detect Cr(vi).

Apart from selectivity, the anti-interference capability is another essential parameter to be thought over when estimating probe performance. Consequently, we examined the changes in fluorescence intensity by adding different metal ions (50  $\mu\text{M}$ ), including  $\text{K}^+$ ,  $\text{Na}^+$ ,  $\text{Ca}^{2+}$ ,  $\text{Mg}^{2+}$ ,  $\text{Ba}^{2+}$ ,  $\text{Ag}^+$ ,  $\text{Zn}^{2+}$ ,  $\text{Mn}^{2+}$ ,  $\text{Co}^{2+}$ ,  $\text{Pd}^{2+}$ ,  $\text{Hg}^{2+}$ ,  $\text{Cd}^{2+}$ ,  $\text{Fe}^{3+}$ ,  $\text{Cr}^{3+}$ ,  $\text{Al}^{3+}$ ,  $\text{Pr}^{3+}$ ,  $\text{Ce}^{4+}$ ,  $\text{F}^-$ ,  $\text{Cl}^-$ ,  $\text{CO}_3^{2-}$ ,  $\text{SO}_4^{2-}$ ,



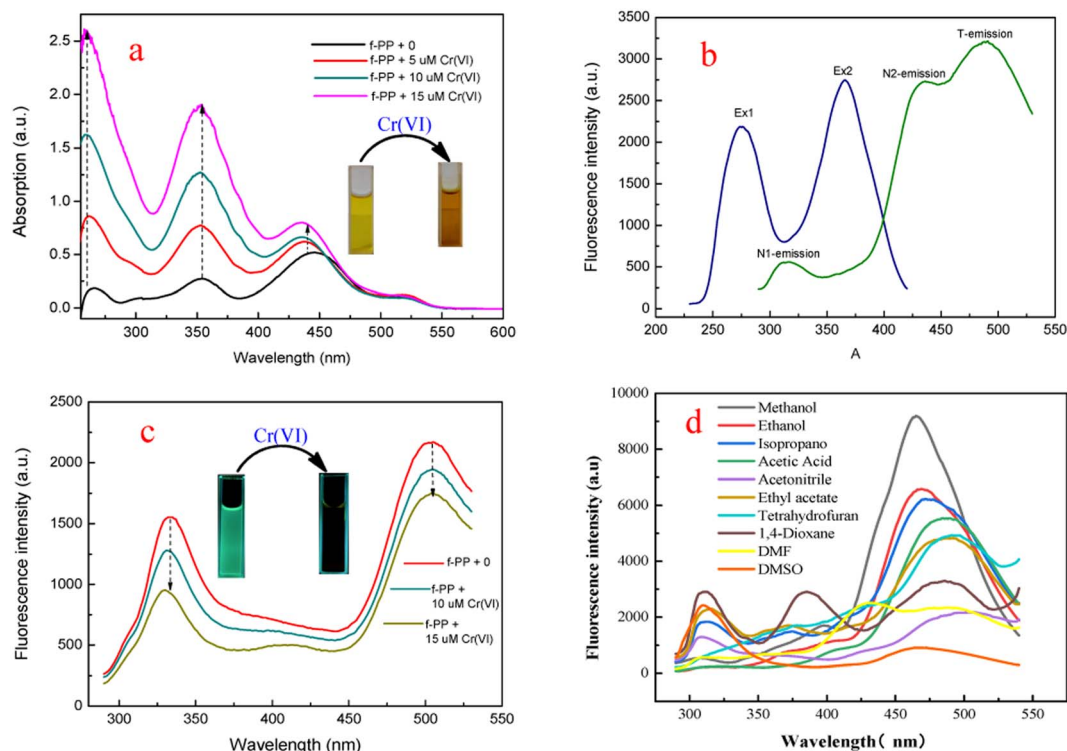


Fig. 2 Absorption and fluorescence spectra of f-PP and the f-PP with the addition of Cr(vi). (a) Absorption spectra of f-PP and the f-PP with the addition of Cr(vi) in DMF-HEPES mixed system (3/7, v/v, pH 7.2). (b) Excitation and fluorescence spectra of f-PP in the same DMF-HEPES system. (c) The fluorescence spectra of f-PP in the presence of different concentrations of Cr(vi). (d) Fluorescence spectra of f-PP in different solvents. Ex = 275 nm.

$\text{NO}_3^-$ , urea, citric acid, glucose, sucrose, methanol and ethanol to the f-PP solutions containing  $20 \mu\text{M}$  Cr(vi) ions, according to the procedure described in the Experimental section. The fluorescence spectra displayed in Fig. 3b suggest that Cr(vi) effectively lowered the fluorescence intensity of f-PP even with the addition of other metal ion species. These results confirmed that the proposed ESIPT probes f-PP could act as a unique sensing.

### 3.4. Condition optimization

In order to fully explore the sensing performance of f-PP, we optimized the reaction conditions. Medium pH is an important factor for the performance of probes because of that the pH of real wastewater samples may vary from one to the other. Therefore, the fluorescent intensity of f-PP and the f-PP with the addition of Cr(vi) was inspected under moderate broad pH. As shown in Fig. 4a, the ESIPT fluorescence of f-PP was weak at acidic and basic pH because of the protonation of  $-\text{NH}_2$  groups at acidic pH and the deprotonation of  $-\text{OH}$  groups on f-PP, resulting to develop “protective shell” with positive (acidic pH) and negative (basic pH) charges on the side chain of f-PP, which can affect ESIPT process, accompanied by fluorescence quenching of f-PP. It is clear that the maximum fluorescence intensity appeared at HEPES pH 7.2, suggesting that f-PP were stable and exhibited maximum intensity at HEPES pH 7.2. From the perspective of the oxidation of Cr(vi),  $\text{Cr}_2\text{O}_7^{2-}$  had strong oxidability in acid medium. Meanwhile in basic solutions  $\text{Cr}_2\text{O}_7^{2-}$  will convert to

$\text{CrO}_4^{2-}$ , which still occur in high valence state Cr(vi) and hold moderate oxidation capacity. Therefore, HEPES pH 7.2 was selected as the optimum pH for sensing Cr(vi).

The influence of reaction time on the fluorescent behavior of f-PP in the presence of Cr(vi) were investigated. The fluorescence spectra of f-PP-containing solutions with the addition of Cr(vi) were recorded at different reaction times from 1.0 to 9.0 min at room temperature. The fluorescence intensity of the f-PP-Cr(vi) mixture was gradually decreased with increasing reaction time extension owing to the oxidation of f-PP, extending the minimum value of fluorescence at 5 min. After 5 min-reaction, the fluorescence intensity of the f-PP-Cr(vi) solutions has hardly decreased again, which stimulates that the oxidation of f-PP reaches to saturation (Fig. 4b). Therefore, 5 min was selected as the best reaction time for the fluorescence quenching of f-PP.

Next, we evaluated the effect of temperature on the oxidation reaction of Cr(vi) with f-PP. As shown Fig. 4c, the fluorescent intensity of the f-PP-Cr(vi) mixed system decreased slowly to the elevated temperature from room temperature to  $45^\circ\text{C}$ . Decidedly, the increased temperature can provide more energy to promote the forward ox-reductive reaction between f-PP and Cr(vi). For the consideration of experimental operation, room temperature was used as the reaction temperature for the fluorescence quenching of f-PP. Finally, the effect of the ratio f-PP/Cr(vi) on the fluorescence quenching was also investigated. Fig. 4d showed that when the ratio of f-PP to Cr(vi) reaches to 1 : 5, a plateau of fluorescence quenching appears. This may



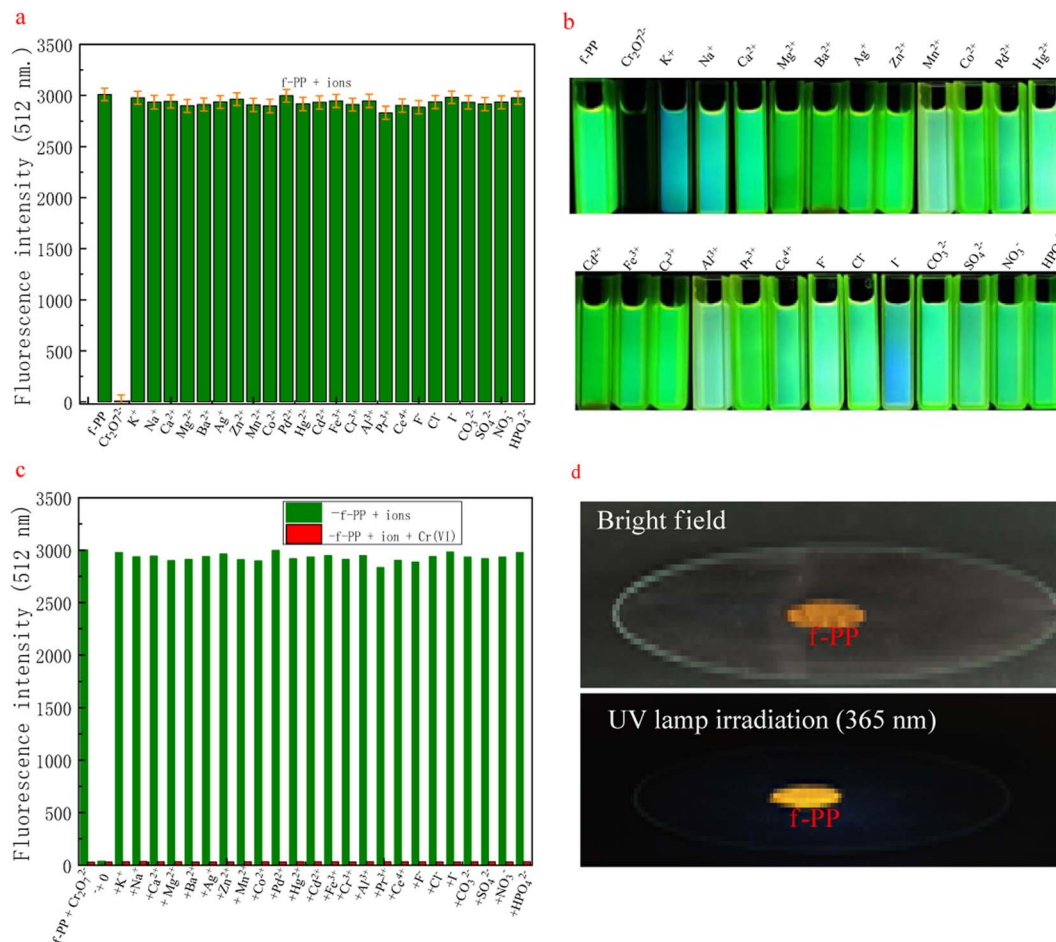


**Fig. 3** Fluorescence change of f-PP upon the addition of 10  $\mu\text{M}$  Cr(VI) and different ions (100  $\mu\text{M}$ ). (a) Fluorescence decrease at 512 nm of f-PP in the presence of Cr(VI) and various species in HEPES-DMF system (10 mM, pH = 7.2, 7 : 3, v/v) at room temperature ( $\lambda_{\text{ex}}$  = 275 nm. Slits: 2.5 nm). (b) The fluorescence images of the probe f-PP with the addition of Cr(VI) and other ions, respectively; (c) red bars represent the f-PP solutions in the presence of Cr(VI) (15  $\mu\text{M}$ ) and various ions (150  $\mu\text{M}$ ); (d) the images of the product f-PP under door light and UV-lamp (365 nm), respectively.

suggest that the structure stability of f-PP destroyed, accompanied with the fluorescence quenching.

### 3.5. Determination of Cr(VI) in real water samples using f-PP

The feasibility of the fluorescent probe f-PP for the detection of Cr(VI) in real water samples was investigated. Firstly, the calibration graph was established by adding different concentrations of Cr(VI) into the f-PP solutions. As shown in Fig. 5a, with the increase of Cr(VI) concentration, the ESIPT emission intensity of f-PP is progressively decreased, and a good linear relationship ( $R^2 = 0.99748$ ) was showed between the fluorescence quenching and the Cr(VI) concentration in the range of 0–40  $\mu\text{M}$  (Fig. 5b). The limit of detection was calculated as 19.5 nM ( $3\sigma/\text{slope}$ ), which is lower than the permissible levels of Cr(VI) in water with 0.95  $\mu\text{M}$  (0.05  $\text{mg L}^{-1}$ ) recommended by the World Health Organization and US Environmental Protection Agency.<sup>44,45</sup> The detection limit of our proposed f-PP based method is lower than that of the reported ones in the literature.<sup>22,46</sup>

Subsequently, the measurements of Cr(VI) in real water samples was carried out with standard addition method. As

shown in Table 1, the concentrations of Cr(VI) in tap water and lake water is undetected. After the addition of fixed Cr(VI) amount, the recoveries of Cr(VI) range from 98.0 to 103.2% with the relative standard deviations (RSD) of 1.75–2.55%. The tracked concentrations of Cr(VI) in each groups are in good agreement with the initial added ones. Besides the above natural water samples, the practicality of f-PP for the detection of Cr(VI) in waste water was also evaluated using f-PP-based probe. The results showed that there are no significant differences for the determination of Cr(VI), indicating the accuracy of our proposed method. These results demonstrated that the ESIPT f-PP as a novel fluorescent probe has application feasibility for the selective determination of Cr(VI) in real water samples.

### 3.6. Application of f-PP to fluorescence imaging of *in vitro* protein

We evaluated the performance of f-PP for protein imaging *in vitro* using the expressed proteins of Mambalgin gene as analytic models. Firstly, the inclusions of the gene transduced



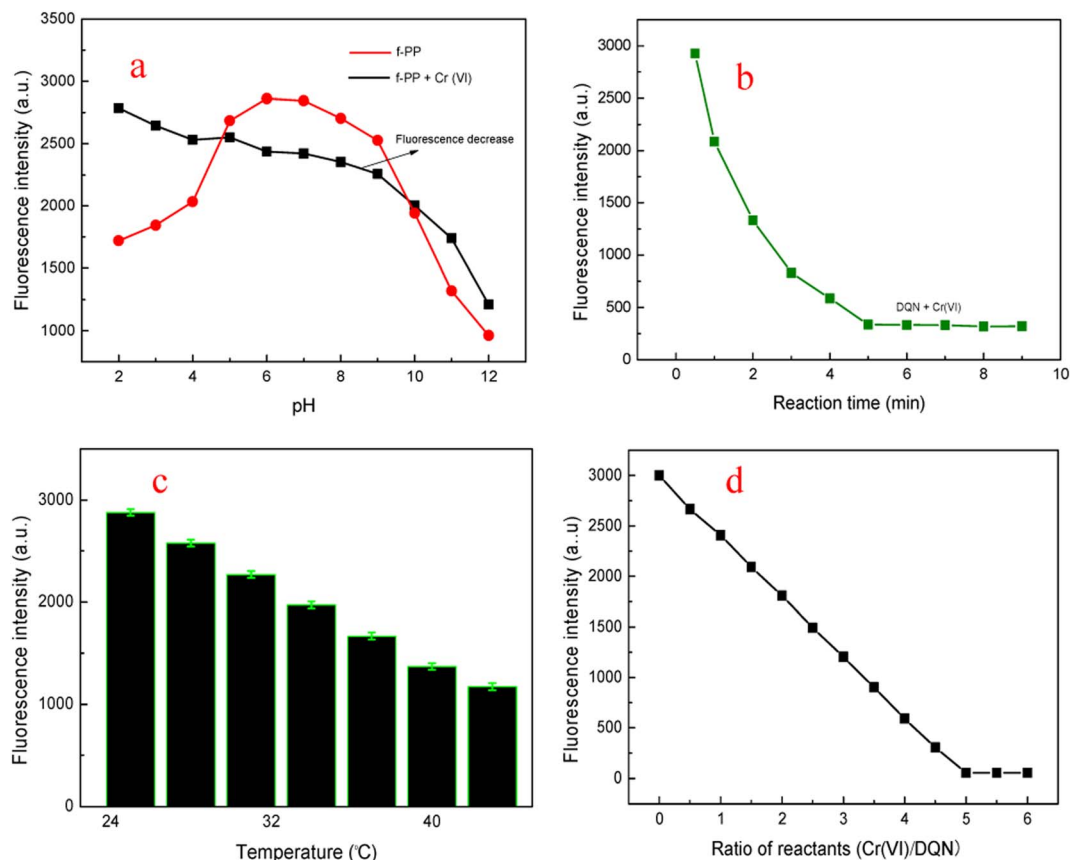


Fig. 4 The effect of reaction conditions on the fluorescent performance of f-PP and f-PP + Cr(VI). (a) pH; (b) reaction time; (c) temperature; (d) ratio of f-PP to Cr(VI). The concentrations of f-PP were  $20 \mu\text{g L}^{-1}$ . Ex = 275 nm; Em = 512 nm.

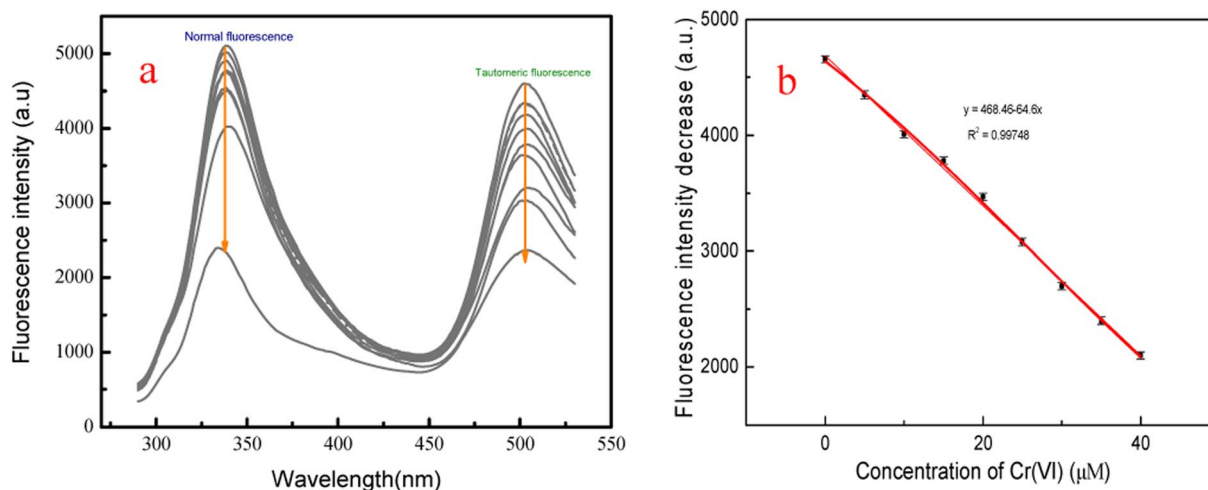


Fig. 5 (a) Fluorescent spectra of  $5 \mu\text{g L}^{-1}$  f-PP in HEPES-DMF buffer (20 mM, HEPES : DMF = 7/3, pH = 7.2, v/v) in the presence of increasing concentrations of Cr(VI) (from top to bottom: 0, 10.0, 15.0, 20.0, 25.0, 30.0, 35.0 and 40  $\mu\text{M}$ ), excited at 275 nm; (b) plot of the fluorescent intensity at 512 nm of f-PP as a function of the concentrations of Cr(VI).

*Escherichia coli* were separated and fixed by sodium dodecyl sulfate-polyacrylamide gel electrophoresis (SDS-PAGE). Next, the electrophoretic gel bands with different proteins were immersed in the f-PP-containing solution for 2 h, followed by

washing three times with PBS. Finally, fluorescence imaging is carried out on the electrophoretic gel bands. As displayed in Fig. 6, f-PP could stain all the proteins which were colored by Coomassie brilliant blue R250 in the electrophoretic gels. These



Table 1 Determination of Cr(vi) in real water samples

Samples	Added ( $\mu\text{M}$ )	Found ( $\mu\text{M}$ )	Recovery (%)	RSD <sup>a</sup> (% , $n = 3$ )
Tap water	2.50	2.45	98.0	1.76
	10.00	10.32	103.2	1.75
	30.00	29.75	99.2	2.29
Lake water	2.50	2.55	102.0	2.55
	10.00	10.21	101.0	1.87
	30.00	30.47	101.6	2.05
Waste water	2.50	2.79	101.5	1.96
	10.00	10.56	103.0	2.25
	30.00	30.74	101.6	1.82

<sup>a</sup> Relative standard deviations (RSD) of measurements are calculated from three independent experiments.

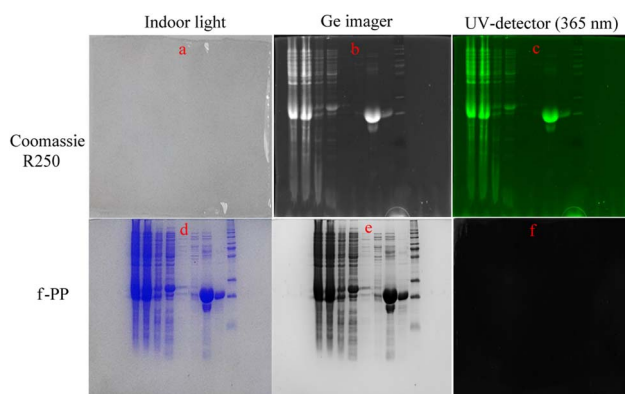


Fig. 6 Fluorescence images of the proteins in SDS-PAGE electrophoresis gel bands stained with f-PP or Coomassie brilliant blue R250. (a–c) The expressed proteins of Mambalgin gene and the inclusions of *Escherichia coli* in electrophoresis gels were stained with f-PP. The samples are as follows: (1) bacterial extract of *Escherichia coli* expressed with Mambalgin gene; (2) the centrifugal supernate of bacterial extract containing Mambalgin; (3) the penetrating fluid of the centrifuged supernate through nickel column; (4) the eluent separated by Ni-column and eluted without imidazole (the first elution); (5) the eluent separated by Ni-column and eluted without imidazole (the second elution); (6) the eluent separated by Ni-column and eluted with 20 mmol L<sup>-1</sup> imidazole; (7) the eluent separated by Ni-column and eluted with 300 mmol L<sup>-1</sup> imidazole; (8) the eluent separated by Ni-column and eluted 500 mmol L<sup>-1</sup> imidazole (the first elution); (9) the eluent separated by Ni-column and eluted 500 mmol L<sup>-1</sup> imidazole (the second elution); (10) protein ruler. (d–f) The same expressed proteins and their protein inclusions in electrophoresis gels were stained with Coomassie brilliant blue R250.

results reveal that the f-PP can anchor the expressed proteins of Mambalgin gene and the other proteins in *Escherichia coli*. Compared to Coomassie brilliant blue R250, the main advantages of f-PP are: (1) it possesses high sensitivity owing to the inherent natures of fluorometry; (2) the reagent dosage is low in the gel chromatography; CBBR250 is usually used at the concentration of 0.1%, while the usage of f-PP is at a relatively lower concentration ( $<10^{-3}$   $\mu\text{M}$ ). (2) The decolorization treatment of the DQN is simpler than that of CBBR250 (immersed in ethanol for 30 min).

## 4. Conclusions

In summary, we have developed an inter-ESPT-based polymeric fluorescent probe for Cr(vi) via a “multicomponent one pot reaction” method. The as-prepared polymeric probe (f-PP) was endowed with multiple inter-ESPT units, enabling it to exhibit the advantage of large Stokes'-shift ([http://www.baidu.com/link?url=68s935ol4-Dyo6BP21y1kfng\\_UREtF55\\_vB2efqU06r\\_pLwp6Ahj6\\_vi-xvEwds-4g-oWwj2JensG60DSCJW0a](http://www.baidu.com/link?url=68s935ol4-Dyo6BP21y1kfng_UREtF55_vB2efqU06r_pLwp6Ahj6_vi-xvEwds-4g-oWwj2JensG60DSCJW0a)), high brightness and good stability. The probe f-PP can show two light ways of normal fluorescence in aprotic solvents and tautomeric fluorescence in protic solvents, respectively. Up on the addition of Cr(vi), the ESIPT fluorescence of f-PP was obviously suppressed, while the presence of other competitive ions could merely cause negligible changes in fluorescence. Taking advantages of Cr(vi) to quench the ESIPT emission of f-PP, we established a novel method for the detection of Cr(vi). The our proposed probe exhibits satisfactory sensitivity and selectivity for determination of Cr(vi) in real water samples, offering the detection limits of 19.5 nM. Given the mentioned advantages, we believe that the inter-ESPT-based polymeric fluorescent probes would have potential applications in environmental and bio-analysis.

## Author contributions

Fuchun Gong: supervision, investigation designed and planned; Jiaoyun Xia: fluorescence spectrum test and analysis. Xiaoling Qin: the design and synthesis of the organic compounds, wrote the manuscript. Pan Ma: characterization of the target molecular and interpretation of the NMR spectra. Lusen Chen: protein staining experiments. Guoqiang Zhou and Lujie Xu: the practical sample detection, cell incubation and fluorescence imaging experiments. All authors read and approved the final manuscript.

## Conflicts of interest

The authors declare that they have no known competing financial interests.

## Acknowledgements

This work was financially supported by the Research Foundation of Education Bureau of Hunan Province (No. 18A141) and the State Key Laboratory of Bio-organic and Natural Product Chemistry (No. SKLBNPC19250).

## References

- M. Elavarasi, S. A. Alex, N. Chandrasekaran and A. Mukherjee, Simple fluorescence-based detection of Cr(III) and Cr(VI) using unmodified gold nanoparticles, *Anal. Methods*, 2014, **6**(24), 9554–9560.
- X. Zhang, M. Zhu, Y. Jiang, X. Wang, Z. Guo, J. Shi, X. Zou and E. Han, Simple electrochemical sensing for mercury ions in dairy product using optimal Cu(II)-based metal-





- organic frameworks as signal reporting, *J. Hazard. Mater.*, 2020, **400**, 123222.
- 3 S. Dey, A. Kumar, P. K. Mondal, K. M. Modi, D. Chopra and V. K. Jain, An oxacalix[4]arene derived dual sensing fluorescent probe for the detection of As(v) and Cr(vi) oxyanions in aqueous media, *Dalton Trans.*, 2020, **49**(22), 7459–7466.
  - 4 T. Madrakian, A. H. Mohammadzadeh, S. Maleki and A. Afkhami, Preparation of polyacrylonitrile nanofibers decorated by N-doped carbon quantum dots: application as a fluorescence probe for determination of Cr(vi), *New J. Chem.*, 2018, **42**(23), 18765–18772.
  - 5 B. K. John, N. John, S. Mathew, B. K. Korah, M. S. Punnoose and B. Mathew, Fluorescent carbon quantum dots as a novel solution and paper strip-based dual sensor for the selective detection of Cr(vi) ions, *Diamond Relat. Mater.*, 2022, **126**, 109138.
  - 6 J. B. Vincent, Elucidating a biological role for chromium at a molecular level, *Acc. Chem. Res.*, 2000, **33**, 503–510.
  - 7 A. Levina, R. Codd, C. T. Dillon and P. A. Lay, Chromium in biology: toxicology and nutritional aspects, *Prog. Inorg. Chem.*, 2002, **51**, 145–250.
  - 8 Z. Wang, X. Wang, W. Niu and L. Feng, A specific fluorescence probe for chromium(vi) anions and its application, *Sens. Actuators, B*, 2017, **244**, 727–731.
  - 9 E. Rossi, M. I. Errea, M. M. F. de Cortalezzi and J. Stripeikis, Selective determination of Cr(vi) by on-line solid phase extraction FI-SPE-FAAS using an ion exchanger resins sorbent: An improvement treatment of the analytical signal, *Microchem. J.*, 2017, **130**, 88–92.
  - 10 S. A. Abayzeed, R. J. Smith, K. F. Webb, M. G. Somekh and C. W. See, Responsivity of the differential-intensity surface plasmon resonance instrument, *Sens. Actuators, B*, 2016, **235**, 627–635.
  - 11 H. Sereshti, M. V. Farahani and M. Baghdadi, Trace determination of chromium(vi) in environmental water samples using innovative thermally reduced graphene (TRG) modified SiO(2) adsorbent for solid phase extraction and UV-vis spectrophotometry, *Talanta*, 2016, **146**, 662–669.
  - 12 N. D. Jayram, D. Aishwarya, S. Sonia, D. Mangalaraj, P. S. Kumar and G. M. Rao, Analysis on superhydrophobic silver decorated copper Oxide nanostructured thin films for SERS studies, *J. Colloid Interface Sci.*, 2016, **477**, 209–2019.
  - 13 H. J. Wang, X. M. Du, M. Wang, T. C. Wang, H. Ou-Yang, B. Wang, M. T. Zhu, Y. Wang, G. Jia and W. Y. Feng, Using ion-pair reversed-phase HPLC ICP-MS to simultaneously determine Cr(III) and Cr(vi) in urine of chromate workers, *Talanta*, 2010, **81**(4), 1856–1860.
  - 14 E. Marguí, C. Fontàs, M. Toribio, M. Guillem, M. Hidalgo and I. Queralt, Determination of Water-Soluble Hexavalent Chromium in Clinker Samples by Wavelength-Dispersive X-ray Fluorescence Spectrometry after Concentration in Activated Layers, *Appl. Spectrosc.*, 2010, **64**(5), 547–551.
  - 15 W. Jin, G. Wu and A. Chen, Sensitive and selective electrochemical detection of chromium(vi) based on gold nanoparticle-decorated titania nanotube arrays, *Analyst*, 2014, **139**(1), 235–241.
  - 16 M. Zheng, Z. Xie, D. Qu, D. Li, P. Du, X. Jing and Z. Sun, On-off-on fluorescent carbon dot nanosensor for recognition of chromium(vi) and ascorbic acid based on the inner filter effect, *ACS Appl. Mater. Interfaces*, 2013, **5**(24), 13242–13247.
  - 17 X. Luo, P. Bai, X. Wang, G. Zhao, J. Feng and H. Ren, Preparation of nitrogen-doped carbon quantum dots and its application as a fluorescent probe for Cr(vi) ion detection, *New J. Chem.*, 2019, **43**(14), 5488–5494.
  - 18 R. Iftikhar, I. Parveen, Ayesha, A. Mazhar, M. S. Iqbal, G. M. Kamal, F. Hafeez, A. L. Pang and M. Ahmadipour, Small organic molecules as fluorescent sensors for the detection of highly toxic heavy metal cations in portable water, *J. Environ. Chem. Eng.*, 2023, **11**(1), 109030.
  - 19 Y. Zhao, Y. Sun, Y. Jiang, S. Song, T. Zhao, Y. Zhao, X. Wang, B. Li, B. Yang and Q. Lin, Fluorescent probe gold nanodots to quick detect Cr(vi) via oxidoreduction quenching process, *Sci. China: Chem.*, 2018, **62**(1), 133–141.
  - 20 W. Qing, K. Chen, Y. Yang, Y. Wang and X. Liu, Cu<sup>2+</sup>-doped carbon dots as fluorescence probe for specific recognition of Cr(vi) and its antimicrobial activity, *Microchem. J.*, 2020, **152**, 104262.
  - 21 L. Sheng, B. Huangfu, Q. Xu, W. Tian, Z. Li, A. Meng and S. Tan, A highly selective and sensitive fluorescent probe for detecting Cr(vi) and cell imaging based on nitrogen-doped graphene quantum dots, *J. Alloys Compd.*, 2020, **820**, 15319.
  - 22 L. M. T. Phan, S. H. Baek, T. P. Nguyen, K. Y. Park, S. Ha, R. Rafique, S. K. Kailasa and T. J. Park, Synthesis of fluorescent silicon quantum dots for ultra-rapid and selective sensing of Cr(vi) ion and biomonitoring of cancer cells, *Mater. Sci. Eng., C*, 2018, **93**, 429–436.
  - 23 J.-B. Qu, S.-H. Li, Y.-L. Xu, Y. Liu and J.-G. Liu, Inherently fluorescent polystyrene microspheres as a fluorescent probe for highly sensitive determination of chromium(vi) and mercury(II) ions, *Sens. Actuators, B*, 2018, **272**, 127–134.
  - 24 A. Tall, F. Antônio Cunha, B. Kaboré, E. S. d'Angeles do, C. Barbosa, U. Rocha, T. O. Sales, M. O. Fonseca Goulart, I. Tapsoba and S. J. Carinhonha Caldas, Green emitting N, P-doped carbon dots as efficient fluorescent nanoprobes for determination of Cr(vi) in water and soil samples, *Microchem. J.*, 2021, **166**, 106219.
  - 25 M. Cao, Y. Li, Y. Zhao, C. Shen, H. Zhang and Y. Huang, A novel method for the preparation of solvent-free, microwave-assisted and nitrogen-doped carbon dots as fluorescent probes for chromium(vi) detection and bioimaging, *RSC Adv.*, 2019, **9**(15), 8230–8238.
  - 26 Y. Deng, W. Niu, Z. Wang and L. Feng, Synthesis, photoelectric properties and application of a polymer fluorescent probe with quinoline and benzene groups, *Sens. Actuators, B*, 2017, **238**, 613–618.
  - 27 A. Sil, S. N. Islam and S. K. Patra, Terpyridyl appended poly(metaphenylene-alt-fluorene)  $\pi$ -conjugated fluorescent polymers: Highly selective and sensitive turn off probes for the detection of Cu<sup>2+</sup>, *Sens. Actuators, B*, 2018, **254**, 618–628.



- 28 Y. Shan, W. Yao, Z. Liang, L. Zhu, S. Yang and Z. Ruan, Reaction-based AIEE-active conjugated polymer as fluorescent turn on probe for mercury ions with good sensing performance, *Dyes Pigm.*, 2018, **156**, 1–7.
- 29 N. Choudhury, B. Ruidas, B. Saha, K. Srikanth, C. Das Mukhopadhyay and P. De, Multifunctional tryptophan-based fluorescent polymeric probes for sensing, bioimaging and removal of  $\text{Cu}^{2+}$  and  $\text{Hg}^{2+}$  ions, *Polym. Chem.*, 2020, **11**(12), 2015–2026.
- 30 S. He, L. Marin and X. Cheng, Novel water soluble polymeric sensors for the sensitive and selective recognition of  $\text{Fe}^{3+}/\text{Fe}^{2+}$  in aqueous media, *Eur. Polym. J.*, 2022, **162**, 110891.
- 31 N. Choudhury, B. Saha, B. Ruidas and P. De, Dual-Action Polymeric Probe: Turn-On Sensing and Removal of  $\text{Hg}^{2+}$ ; Chemosensor for  $\text{HSO}_4^-$ , *ACS Appl. Polym. Mater.*, 2019, **1**(3), 461–471.
- 32 D. Giri, A. Bankura and S. K. Patra, Poly(benzodithienimidazole-alt-carbazole) based  $\pi$ -conjugated copolymers: Highly selective and sensitive turn-off fluorescent probes for  $\text{Hg}^{2+}$ , *Polymer*, 2018, **158**, 338–353.
- 33 L. Feng, Y. Deng, X. Wang and M. Liu, Polymer fluorescent probe for  $\text{Hg}(\text{II})$  with thiophene, benzothiazole and quinoline groups, *Sens. Actuators, B*, 2017, **245**, 441–447.
- 34 S. W. Chen, X. Chen, Y. Li, Y. Yang, Y. Dong, J. Guo and J. Wang, Polydiacetylene-based colorimetric and fluorometric sensors for lead ion recognition, *RSC Adv.*, 2022, **12**(34), 22210–22218.
- 35 M. Gupta, S. Sahana, V. Sharma and P. K. Bharadwaj, Benzothiazole integrated into a cryptand for ESIPT-based selective chemosensor for  $\text{Zn}(\text{II})$  ions, *Dalton Trans.*, 2019, **48**(22), 7801–7808.
- 36 W. Feng, G. Fu, Y. Huang, Y. Zhao, H. Yan and X. Lü, ESIPT-capable  $\text{Eu}^{3+}$ -metallopolymer with colour-tunable emission for selective visual sensing of  $\text{Zn}^{2+}$  ion, *J. Mater. Chem. C*, 2022, **10**(3), 1090–1096.
- 37 A. I. Costa, P. D. Barata, C. B. Fialho and J. V. Prata, Highly sensitive and selective fluorescent probes for  $\text{Cu}(\text{II})$  detection based on calix[4]arene-oxacyclophane architectures, *Molecules*, 2020, **25**(10), 2456.
- 38 H. Diao, L. Guo, W. Liu and L. Feng, A novel polymer probe for  $\text{Zn}(\text{II})$  detection with ratiometric fluorescence signal, *Spectrochim. Acta, Part A*, 2018, **196**, 274–280.
- 39 X. Wang, C. Zhang, Y. Zhang, J. Sun, L. Cao, J. Ji and F. Feng, Facile crosslinking of polythiophenes by polyethylenimine via ester aminolysis for selective  $\text{Cu}(\text{II})$  detection in water, *Biosens. Bioelectron.*, 2018, **109**, 255–262.
- 40 D. Luo, S. G. Liu, N. B. Li and H. Q. Luo, Water-soluble polymer dots formed from polyethylenimine and glutathione as a fluorescent probe for mercury(II), *Mikrochim. Acta*, 2018, **185**(6), 284.
- 41 Y. Zhu, X. Gong, Z. Li, X. Zhao, Z. Liu, D. Cao and R. Guan, A simple turn-on ESIPT and PET-based fluorescent probe for detection of  $\text{Al}(\text{III})$  in real-water sample, *Spectrochim. Acta, Part A*, 2019, **219**, 202–205.
- 42 D. Jiang, M. Zheng, X. Yan, B. Huang, H. Huang, T. Gong, K. Liu and J. Liu, A “turn-on” ESIPT fluorescence probe of 2-(aminocarbonyl)phenylboronic acid for the selective detection of  $\text{Cu}(\text{II})$ , *RSC Adv.*, 2022, **12**(48), 31186–31191.
- 43 Y. Zhang, Z. Li, Q. Sun, Z. Li, Y. Zhi, R. Nie, H. Xia, Y. Yu and X. Liu, Light-Emitting Conjugated Organic Polymer as an Efficient Fluorescent Probe for  $\text{Cu}^{2+}$  Ions Detection and Cell Imaging, *Macromol. Rapid Commun.*, 2021, **42**(19), 2100469.
- 44 A. Mahapatra, B. G. Mishra and G. Hota, Studies on electro-spun alumina nanofibers for the removal of chromium(VI) and fluoride toxic ions from an aqueous system, *Ind. Eng. Chem. Res.*, 2013, **52**(4), 1554–1561.
- 45 F.-M. Li, J.-M. Liu, X.-X. Wang, L.-P. Lin, W.-L. Cai, X. Lin, Y.-N. Zeng, Z.-M. Li and S.-Q. Lin, Non-aggregation based label free colorimetric sensor for the detection of  $\text{Cr}(\text{VI})$  based on selective etching of gold nanorods, *Sens. Actuators, B*, 2011, **155**(2), 817–822.
- 46 Y. Wang, X. Hu, W. Li, X. Huang, Z. Li, W. Zhang, X. Zhang, X. Zou and J. Shi, Preparation of boron nitrogen co-doped carbon quantum dots for rapid detection of  $\text{Cr}(\text{VI})$ , *Spectrochim. Acta, Part A*, 2020, **243**, 118807.

